Anomalous spin polarization of GaAs two-dimensional hole systems

R. Winkler,[1,2] E. Tutuc,[2] S. J. Papadakis,[2] S. Melinte,[2] M. Shayegan,[2] D. Wasserman,[2] and S. A. Lyon[2]
[1]*Institut für Festkörperphysik, Universität Hannover, Appelstrasse 2, D-30167 Hannover, Germany*
[2]*Department of Electrical Engineering, Princeton University, Princeton, New Jersey 08544, USA*
(Received 14 June 2005; published 11 November 2005)

We report measurements and calculations of the spin-subband depopulation, induced by a parallel magnetic field, of dilute GaAs two-dimensional (2D) hole systems. The results reveal that the shape of the confining potential dramatically affects the values of an in-plane magnetic field at which the upper spin subband is depopulated. Most surprisingly, unlike 2D electron systems, the carrier-carrier interaction in 2D hole systems does not significantly enhance the spin susceptibility. We interpret our findings using a multipole expansion of the spin density matrix, and suggest that the suppression of the enhancement is related to the holes' band structure and effective spin $j=3/2$.

DOI: 10.1103/PhysRevB.72.195321 PACS number(s): 73.50.−h, 71.70.Ej, 73.43.Qt

I. INTRODUCTION

It was first pointed out by Janak that for a two-dimensional electron system (2DES) in a static magnetic field the exchange interaction acts like an effective magnetic field (in addition to the applied field) so that the Zeeman energy splitting is enhanced.[1] Recently, the Zeeman splitting and spin susceptibility of interacting 2D carrier systems have been a subject of renewed interest,[2–18] fueled by the promise of a paramagnetic to ferromagnetic ground state transition at very low densities,[19,20] and the possibility that the spin polarization is related to the apparent metal-insulator transition in dilute 2D systems.[21] Experiments have mostly focused on determining the spin susceptibility from magnetotransport,[2–9] and magnetization[10] measurements. The results generally show that the spin susceptibility of 2DESs in different materials, e.g., Si,[2–5,10] GaAs,[6,7] and AlAs[8,9] increases as the density is reduced, one report[3] even suggesting a ferromagnetic instability at the lowest densities.

Lately, the spin polarization of GaAs 2D *hole* systems (2DHSs) has become the subject of intensive research[11–17] because the holes have a larger effective mass (than electrons) so that they can be made effectively more dilute while maintaining high quality. Furthermore, the spin polarization of holes is important in the context of ferromagnetic semiconductors such as GaMnAs, where it is known that the ferromagnetism is mediated by the itinerant valence band holes.[22,23] We show here that the spin susceptibility of 2DHSs depends dramatically on the shape of the confining potential. Moreover, we find that, in contrast to their 2D electron counterparts, dilute 2DHSs exhibit no significant enhancement of the spin susceptibility as compared with calculations that neglect exchange correlation. We will argue that this surprising behavior is related to the holes' band structure and the fact they have effective spin $j=3/2$ rather than $j=1/2$, which is the case for electrons.

II. SAMPLE PARAMETERS AND EXPERIMENTAL DETAILS

Four samples from different wafers, including two GaAs/AlGaAs heterojunctions and two GaAs quantum wells (QWs) flanked by AlGaAs barriers, were investigated in this study (Table I). Depending on their substrate orientation and carrier type, our samples were either Be doped (samples H, Q1) or Si doped (Q2, A). All samples were fitted with metal front and back gates to control their density as well as the electric field perpendicular to the 2D systems. We made measurements in ^{3}He or dilution refrigerators of temperature $T=0.3$ K and in magnetic fields up to 25 T.

III. EXPERIMENTAL RESULTS FOR (001) 2D HOLES

In Fig. 1(a) we show the longitudinal resistivity ρ_{xx} versus in-plane magnetic field $B_\parallel$ for samples H and Q1, both measured at a density of $n=3.7\times10^{10}$ cm^{-2}. The data shows a positive magnetoresistance with a marked change in functional form above the magnetic field B_d that reflects the complete depopulation of the minority spin subband.[2,13] In Fig. 1(a), B_d is marked by arrows. Remarkably, the field B_d depends greatly on the shape of the confining potential. Indeed, we have $B_d\simeq10.6$ T for sample H and $B_d\simeq20.5$ T for sample Q1, even though the data were taken at the *same* density.

In Fig. 1(c) we show B_d in sample H when the electric field $\mathcal{E}$ across the junction is varied by means of front and back gates such that n is kept constant at 4.5×10^{10} cm^{-2}. The field B_d increases significantly with increasing $\mathcal{E}$. In Fig. 2(a) we show the measured B_d vs n for sample H. The values of B_d depend rather sensitively on whether n is changed by means of a front or back gate.

TABLE I. Typical densities n (in 10^{10} cm^{-2}) and mobilities μ (in m^2/V s) of the samples used in this study.

Sample	Carriers	Structure	Substrate	n	μ
H	Holes	Heterojunction	(001)	5.3	30
Q1	Holes	150 Å wide QW	(001)	4.8	11
Q2	Holes	200 Å wide QW	(113)A	6.8	55[a]
A	Electrons	Heterojunction	(001)	3.0	48

[a]μ for $\mathbf{I}\|[33\bar{2}]$. For $\mathbf{I}\|[\bar{1}10]$ we have $\mu=35$ m^2/V s.

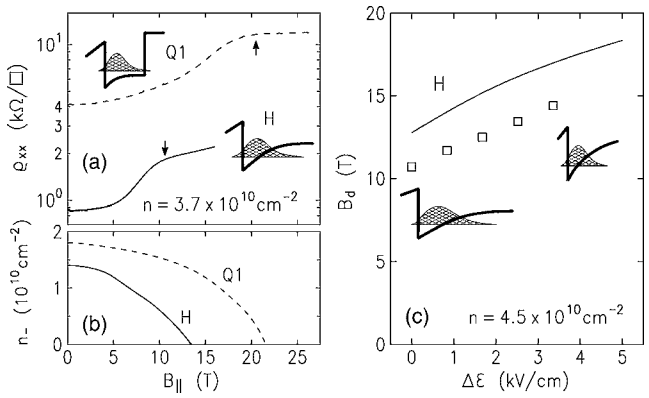

FIG. 1. (a) Longitudinal resistivity ρ_{xx} versus in-plane magnetic field $B_\parallel$ measured at $T=0.3$ K for 2D hole samples, H and Q1, at the same density $n=3.7\times10^{10}$ cm^{-2}. The depopulation fields B_d are marked by arrows. (b) Calculated density n_- in the minority spin subband of samples H and Q1 as a function of $B_\parallel$. (c) Measured (squares) and calculated (solid line) depopulation field B_d versus change $\Delta\mathcal{E}$ of the electric field in sample H for constant density $n=4.5\times10^{10}$ cm^{-2}.

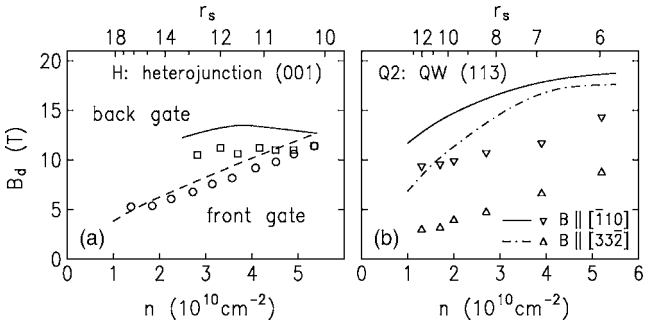

FIG. 2. Measured (symbols) and calculated (lines) depopulation field B_d as a function of n for samples (a) H and (b) Q2. The measurements were performed at $T=0.3$ K. In (a), for the solid line and squares (dashed line and circles) n was varied via a back (front) gate. In (b) the different symbols refer to $\boldsymbol{B}\|[\bar{1}10]$ and $\boldsymbol{B}\|[33\bar{2}]$ as indicated. The upper horizontal axes show the calculated density parameter r_s for the corresponding n. In (a) we used $r_s(n)$ for the front gate.

IV. CALCULATIONS AND DISCUSSIONS

In order to explain the experimental results of Figs. 1 and 2, we have performed parameter-free calculations in the multiband envelope-function and self-consistent Hartree approximations for the quasi-2D system.[7,24] Figure 1(b) shows the calculated density n_- in the minority spin subband as a function of $B_\parallel$. The lines in Figs. 1(c) and 2 show the calculated B_d for the corresponding experiments.[25] The calculations reproduce the different behavior of samples H and Q1 in satisfactory agreement with experiment.

A. Confinement potential dependence of B_d

As we discuss in the next section, the close agreement between the experimental and calculated B_d in Figs. 1 and 2(a) is very surprising because the calculations do not take exchange-correlation effects into account. Such effects are indeed dominant for 2D *electron* systems[1–10,18,26–28] that are as dilute as the 2DHSs of Figs. 1 and 2(a). Before elaborating on this aspect of our results, however, we first discuss the remarkably strong dependence of B_d on the confining potential. For an ideal, strictly 2D system with effective mass m^* and effective g factor g^* we have $B_d\propto1/(m^*g^*)$, independent of the shape of the confining potential. To understand the surprising results in Figs. 1 and 2, we will first concentrate on the Zeeman splitting, which gives rise to the dominant contribution of the confinement dependence of B_d in 2DHSs. Then we discuss the effect of $B_\parallel$ on the orbital motion.

Unlike electrons in the conduction band that have spin-1/2, holes in the uppermost valence band are characterized by an effective spin-3/2 (Ref. 24). Subband quantization in 2DHSs yields a quantization of angular momentum with z component $m=\pm3/2$ for the heavy holes (HHs) and $m=\pm1/2$ for the light holes (LHs). In our samples, only the lowest HH subband is occupied. The quantization axis of angular momentum that is enforced by HH-LH splitting points perpendicular to the 2D plane. The Zeeman energy splitting due to $B_\parallel$ thus competes with the HH-LH splitting and it is well known that the $B_\parallel$-linear Zeeman splitting of HH states is suppressed.[29,30] [The simple model of Ref. 29 yields $B_d\simeq250$ T for the systems in Fig. 1(a).] In the following we will discuss why the depopulation fields B_d observed in real 2DHSs are much smaller than what these arguments suggest.

The dispersion of HH states is known to be highly nonparabolic as a consequence of HH-LH coupling.[24] Therefore, the suppression of Zeeman splitting linear in $B_\parallel$ is merely the lowest-order effect in a Taylor expansion of the spin-split dispersion $E_\sigma(\mathbf{k}_\parallel,B_\parallel)$ of HH states as a function of the (canonical) wave vector $\mathbf{k}_\parallel$, $B_\parallel$, and spin index σ. Mixed higher-order terms proportional to $B_\parallel$ and $\mathbf{k}_\parallel$ give rise to an average Zeeman splitting of the occupied hole states that is approximately linear in $B_\parallel$. Thus we find that B_d is generally much smaller than the value one would expect if the $B_\parallel$-linear Zeeman splitting were suppressed. This is also consistent with previous experimental data for 2DHSs that were interpreted ignoring completely the suppression of $B_\parallel$-linear Zeeman splitting in HH systems.[11–15]

Now we can understand why the Zeeman energy splitting in 2DHSs depends sensitively on the shape of the confining potential. The mixed higher-order terms that are responsible for the Zeeman energy splitting $E_Z(B_\parallel)$ of HH systems compete with the HH-LH splitting. The latter depends sensitively on the shape of the confining potential so that we have here a tool to tune $E_Z(B_\parallel)$ of 2DHSs. In narrow quasi-2D HH systems we have a large HH-LH splitting so that the Zeeman energy splitting is reduced, giving rise to a large B_d. We get a large $E_Z(B_\parallel)$ (a small B_d) in wide systems. We can define $E_Z(B_d)$ as the energy difference between the Fermi energy and the subband edge at B_d. In the wide heterojunction of Fig. 1(b), the calculated $E_Z(B_d)$ is 0.44 meV, significantly larger than $E_Z(B_d)=0.26$ meV in the narrower QW, despite the smaller value of B_d in the heterojunction. Similarly, the increase of B_d with increasing $\Delta\mathcal{E}$ in Fig. 1(c) reflects the change of the HH-LH splitting in the system.

Next we discuss the effect of $B_\parallel$ on the orbital motion. In general,[31] the mass of the particles in quasi-2D systems increases as a function of $B_\parallel$, which reflects the fact that, ultimately, for large $B_\parallel$ resulting in a magnetic length comparable to the width of the quasi-2D system, the particle states become dispersionless Landau levels. Obviously, this effect depends on the thickness of the quasi-2D system, and it has been shown that B_d in wide quasi-2D *electron* systems is much smaller than B_d in narrow 2DESs.[7] We will argue next that the mass enhancement does not explain, however, the results in Figs. 1 and 2(a).

Our numerical calculations show, in agreement with the 2DESs results,[7] that the mass enhancement at small $B_\parallel$ is smaller in the QW than in the heterojunction. However, m^* in 2DHSs increases highly nonlinearly as a function of $B_\parallel$, which is particularly important for the QW with the larger B_d. Thus, we find that at B_d the mass enhancement in the narrower 2DHS of the QW is larger than in the wide 2DHS of the heterojunction. We note that at B_d the mean kinetic energy equals approximately half the Zeeman energy splitting $E_Z(B_d)$ so that for Fig. 1(b) the mass enhancement can be inferred from the E_Z values quoted above [see also Eq. (1) below].

The anomalous enhancement of m^* at B_d with decreasing width of the quasi-2D HH system depends sensitively on the system parameters such as the density and the shape of the confining potential. For the parameters in Fig. 1(c), m^* at B_d is approximately independent of $\Delta\mathcal{E}$ (despite the significant change of B_d), i.e., the increase of B_d with $\Delta\mathcal{E}$ is essentially only due to the decrease of the Zeeman splitting discussed above. For about two times the largest field $\Delta\mathcal{E}$ we could reach experimentally, one enters the regime when m^* at B_d starts to increase with $\Delta\mathcal{E}$. We remark that a purely experimental analysis in order to discriminate between the orbital effect of $B_\parallel$ and the $B_\parallel$ induced Zeeman splitting would be very difficult for 2DHSs due to the fact that the Zeeman splitting of 2D holes also depends on the confining potential, see above.

B. Lack of spin susceptibility enhancement for (001) 2D holes

A most remarkable aspect of the results in Figs. 1 and 2(a) is the reasonable *quantitative* agreement between the experimental data and the calculations. This is particularly puzzling because many-particle effects beyond the Hartree approximation (i.e., exchange-correlation effects) were not taken into account. This is in sharp contrast to the case of dilute 2DESs, for which it is known that exchange correlation significantly increases the spin susceptibility when n is reduced.[1–10,18,26–28] To quantify this point we show in Fig. 3 the ratio $B_d^0/B_d^{\rm exp}$ of the depopulation field B_d^0, calculated neglecting exchange correlation, to the experimentally measured field $B_d^{\rm exp}$ for a 2DES (squares)[32] and the 2DHS (circles) in sample H. The ratio thus reflects the enhancement of the spin susceptibility at B_d due to exchange correlation. Our results are plotted as a function of the dimensionless density parameter r_s defined as the average interparticle spacing measured in units of the effective Bohr radius $a_{\rm B}^*$, $r_s \equiv 1/(a_{\rm B}^*\sqrt{\pi n})$.

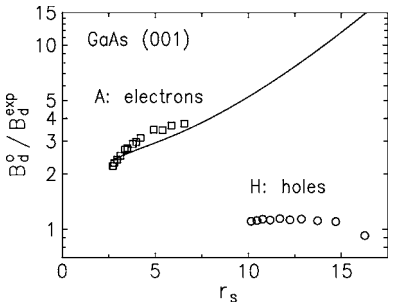

FIG. 3. Ratio $B_d^0/B_d^{\rm exp}$ of the depopulation field B_d^0 calculated neglecting exchange correlation to the measured field $B_d^{\rm exp}$ for a 2DES (squares) and a 2DHS (circles) in GaAs (001) heterojunctions plotted versus the density parameter r_s. In both cases, n was varied via a front gate. For electrons, the solid line shows the ratio $B_d^0/B_d^{\rm xc}$, where $B_d^{\rm xc}$ was calculated, taking into account exchange correlation (Refs. 7 and 28).

For the 2DES in Fig. 3, the ratio $B_d^0/B_d^{\rm exp}$ is between 2 and 4 and, as expected, it increases with r_s. We also remark that for electrons the experimentally observed reduction of B_d is in reasonable quantitative agreement with numerical calculations that take exchange correlation into account. To illustrate this point, the solid line in Fig. 3 shows the ratio $B_d^0/B_d^{\rm xc}$, where $B_d^{\rm xc}$ was calculated in the framework of spin-density-functional theory using a parametrization of the polarization-dependent exchange-correlation potential that was recently obtained by means of quantum Monte Carlo calculations.[7,28] For the 2DHS, on the other hand, the expected enhancement of the spin susceptibility and $B_d^0/B_d^{\rm exp}$ ratio is conspicuously absent in Fig. 3. Note that, because of their larger effective mass compared to GaAs electrons ($m^* \simeq 0.25$ compared to $m^* = 0.067$; here m^* is given in units of the free-electron mass), 2DHSs have significantly larger r_s, and are thus effectively much more dilute. Nonetheless, the ratio $B_d^0/B_d^{\rm exp}$ remains close to unity up to the largest values of r_s, where a greater than tenfold enhancement is expected.

Before discussing possible reasons for this anomalous behavior of 2DHSs, we make remarks regarding the effective mass m^* which enters $a_{\rm B}^*$ and thus determines r_s. For holes, m^* is not uniquely defined. As discussed above, the HH dispersions are typically nonparabolic, meaning that m^* depends on energy, and therefore on n and the confinement potential. Moreover, the HH systems have a large Rashba and Dresselhaus spin splitting at $B=0$ (Ref. 24), leading to two energy versus wave vector ($\mathbf{k}_\parallel$) dispersions with different curvatures and effective masses, m_+^* and m_-^*. Commonly, values of m^* between about 0.2 and 0.4 are used for holes in GaAs.[11,14,15,24,33] Here we adopt a simple definition for an average effective mass $\langle m^* \rangle$:

$$\langle m^* \rangle = \hbar^2 \pi n / (2\langle E_k \rangle), \tag{1}$$

where $\langle E_k \rangle$ is the mean kinetic energy per particle. Figure 4(a) shows the calculated density parameter r_s in sample H, when n is changed by means of a front or back gate. Note that for a single, parabolic dispersion with an effective mass m^*, the mass $\langle m^* \rangle$ as defined in Eq. (1) properly reduces to m^* and is independent of n. For the 2DHS, on the other hand,

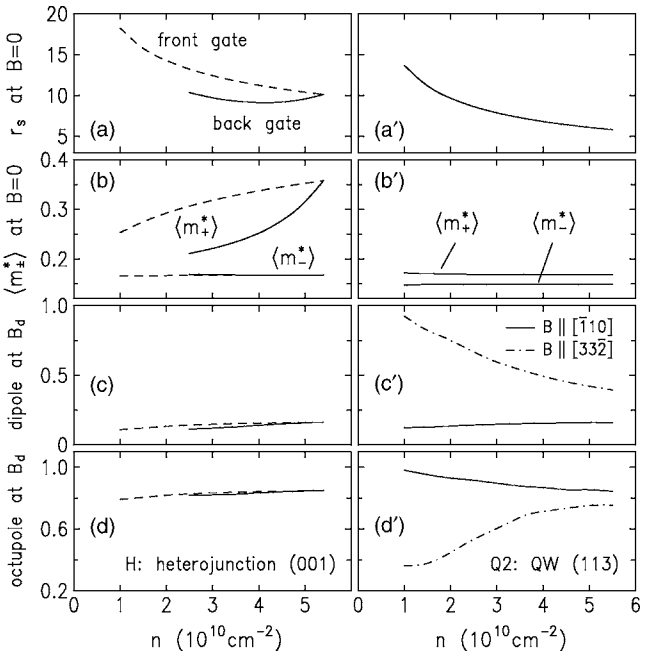

FIG. 4. Calculated density parameter r_s, average effective mass $\langle m_{\pm}^{*}\rangle$, normalized dipole, and octupole moments (Ref. 34) versus n for samples H and Q2. Line styles have the same meaning as in Fig. 2.

$\langle m^{*}\rangle$, in general, depends sensitively not only on n but also on the system's parameters, such as the thickness of the 2DHS and on the applied electric and magnetic fields, as discussed above. If we take into account Rashba and Dresselhaus spin splitting,[24] then we get, similar to Eq. (1), effective masses $\langle m_{\pm}^{*}\rangle$ for each spin subband. To illustrate this effect, we show $\langle m_{\pm}^{*}\rangle$ for sample H in Fig. 4(b). We emphasize that the main conclusion of our work, namely the lack of enhancement of the spin susceptibility with increasing diluteness, is not affected by the specific values of m^{*} used to define r_s: it is clear in Fig. 3 that if r_s were changed by a factor of 2 or 3, there would still exist a large discrepancy between the experimental hole data and the expected enhancement.

In Fermi liquid theory, the enhancement of the spin susceptibility is proportional to the product $m_{\mathrm{QP}}^{*}g_{\mathrm{QP}}^{*}$, where m_{QP}^{*} is the effective mass and g_{QP}^{*} is the effective g factor of the quasiparticles at the Fermi energy. Recently, several authors studied the many-body enhancement of m_{QP}^{*} in electron systems by analyzing the temperature dependence of Shubnikov-de Haas oscillations, see, e.g., Ref. 35 and references therein. These experiments yield the effective mass m_{QP}^{*} of the particles at the Fermi energy. For electron systems with a parabolic energy dispersion, m_{QP}^{*} is indeed a parameter characterizing all electrons in the system. For hole systems with a highly nonparabolic energy dispersion, this mass will be a pronounced function of the Fermi energy as it changes due to the in-plane magnetic field. The proper interpretation of an experimental measurement of m_{QP}^{*} as a function of B is therefore rather problematic. In the present work we thus focus on the spin susceptibility when discussing many-body effects.

C. Anomalous spin polarization of 2D holes

Why do dilute 2DHSs *not* show a significant enhancement of the spin susceptibility? Using a recently developed multipole expansion of the spin density matrix[16] we argue in the remainder of this paper that the $j=3/2$ hole spin is the likely culprit. For 2DESs with spin-1/2, it is well known that the mean Coulomb energy $\langle E_c\rangle$ per particle can be completely characterized using n and (the magnitude of) the spin polarization $\boldsymbol{\zeta}$ as independent parameters.[26] This is because the 2×2 spin density matrix of spin-1/2 systems can be decomposed into four independent terms: n (a monopole) and the three components of the spin polarization vector $\boldsymbol{\zeta}$ (a dipole).[16] In the Hartree-Fock (HF) approximation, the direct part of the Coulomb energy $\langle E_c^{\mathrm{HF}}\rangle$ cancels the potential of the positive background so that only the exchange term $\langle E_x\rangle$ remains,[36,37]

$$\langle E_c^{\mathrm{HF}}\rangle = \langle E_x\rangle = -\frac{2e^2}{3\pi}\sqrt{2\pi n}[(1+\zeta)^{3/2}+(1-\zeta)^{3/2}]. \quad (2)$$

The Coulomb energy $\langle E_c^{\mathrm{HF}}\rangle$ is thus proportional to $\sqrt{n}$. Higher-order terms in a series expansion for $\langle E_c\rangle(n,\zeta)$ of 2DESs were calculated in Ref. 26. $\langle E_c\rangle$ was calculated numerically in, e.g., Refs. 27 and 28.

The 4×4 spin density matrix of $j=3/2$ 2DHSs, on the other hand, can be decomposed into four multipoles, where the monopole is the density n, the dipole corresponds to the spin polarization at $B>0$, the quadrupole reflects the HH-LH splitting, and the octupole is a unique feature of $j=3/2$ hole systems at $B>0$ (Ref. 16). For sample H, the normalized dipole and octupole at B_d are shown in Figs. 4(c) and 4(d) (Ref. 34). Unlike 2DESs, the dipole at B_d is much smaller than unity, i.e., despite the fact that only one spin subband is occupied at B_d, the system is only weakly spin polarized. This result[17] is an immediate consequence of the suppression of $B_{\parallel}$-linear Zeeman splitting[29,30] discussed above. The octupole can be interpreted as a new "spin degree of freedom" of spin-3/2 hole systems at $B>0$, which does not exist for the more familiar case of spin-1/2 electron systems. When the spin polarization is suppressed for an in-plane magnetic field, the 2D HH systems acquire instead a large octupole moment,[38] as visible in Fig. 4(d). The quadrupole is always close to unity because the HH-LH mixing is small in the systems considered here. Therefore, the quadrupole is not shown in Fig. 4. By definition, these four multipoles provide a set of *independent* parameters that can be used to parametrize the Coulomb energy $\langle E_c\rangle$ of spin-3/2 systems, similar to $\langle E_c\rangle(n,\zeta)$ in spin-1/2 systems.[39] However, the series expansion is presently not known and its calculation represents a formidable task. Our study indicates that the series expansion of $\langle E_c\rangle$ of spin-3/2 2DHSs is qualitatively different from $\langle E_c\rangle(n,\zeta)$ of spin-1/2 2DESs.

The HF exchange energy $\langle E_x\rangle$ of 2D HH systems at $B=0$ is the same as $\langle E_x\rangle$ of spin-1/2 2DESs because Eq. (2) requires only that the eigenstates of the two spin subbands for the same $\mathbf{k}_{\parallel}$ are orthogonal.[36] For an HH system, the main effect of a perpendicular magnetic field $B_{\perp}$ is a spin polarization (a dipole), whereas an in-plane field $B_{\parallel}$ usually gives

rise to an octupole moment.[16,38] The spin density matrices of 2D HH systems at $B_\perp > 0$ and $B_\parallel > 0$ are thus qualitatively different. However, the HF exchange energy does not distinguish between these cases and always leads to the same enhancement of the exchange energy as in 2DESs. We note that different results can be obtained for $\langle E_x \rangle$ when HH-LH mixing is significant.[40] Also, different results are obtained for $\langle E_c \rangle$ in higher-order perturbation theory when the more complicated energy dispersion must be taken into account. These are the reasons why the well-established results for exchange-correlation in dilute spin-1/2 2DESs cannot easily be transferred to spin-3/2 2DHSs.

V. RESULTS FOR (113) 2D HOLES

We extend our investigation by comparing the results for sample H with the data for Q2, a QW grown on a (113)A GaAs substrate. Figure 2(b) shows B_d vs n for Q2. The field B_d strongly depends on whether $\mathbf{B}_\parallel$ is applied in the in-plane crystallographic directions $[\bar{1}10]$ or $[33\bar{2}]$ (Ref. 41). The right column of Fig. 4 shows r_s, $\langle m_\pm^* \rangle$, the dipole and the octupole moments calculated for Q2. For this sample, when $\mathbf{B}_\parallel$ is applied parallel to $[33\bar{2}]$, the measured B_d is well below the calculated value. It is remarkable that for this particular geometry, the octupole remains small, but the 2DHS develops a large dipole moment [Figs. 4(c′) and 4(d′)], similar to 2DESs in a $\mathbf{B}_\parallel$ (Ref. 42). This observation suggests that the spin susceptibility is enhanced by many-particle effects only when the magnetic field gives rise to a spin polarization. On the other hand, Figs. 2 and 4 suggest that there is no significant enhancement in $j=3/2$ 2DHSs with a large octupole but a small dipole moment.

VI. SUMMARY AND CONCLUSIONS

We have shown that the spin susceptibility of dilute GaAs 2DHSs in an in-plane magnetic field $B_\parallel$ depends sensitively on the shape of the confining potential. Most remarkably, the spin susceptibility is not significantly enhanced as compared with calculations that neglect the carrier-carrier interaction. This is in sharp contrast to dilute electron systems for which it is known that many-body effects greatly enhance the spin susceptibilty. Using a multipole expansion of the spin density matrix, we have argued that the suppression of the enhancement is related to the holes' band structure and effective spin $j=3/2$.

Our findings have important implications for the quantum phase diagram of dilute 2DHSs. In dilute *electron* systems, the exchange-correlation enhancement of the spin susceptibility can be considered a precursor for the ferromagnetic liquid, which is expected to be the ground state of ultralow density 2DESs with $r_s \gtrsim 26$ (Ref. 28). The extra multipoles of 2DHSs provide new possibilities for the ground state of hole systems to respond to external perturbations such as a magnetic field, thus leading to a richer phase diagram than in spin-1/2 electron systems.[39] However, our results suggest that a ferromagnetic phase (i.e., a fully spin-polarized phase with a maximum dipole moment) is often not favored in dilute 2DHSs. This could also have important implications for ferromagnetic semiconductors such as GaMnAs, where it is known that the ferromagnetism is mediated by the itinerant spin-3/2 holes in the valence band.[22,23] In itinerant ferromagnets it is the polarization-dependent competition between the Coulomb energy and the kinetic energy of the interacting carriers that controls the ferromagnetic transition.

ACKNOWLEDGMENTS

We thank BMBF, DOE, NSF, and ARO for support, and D. C. Tsui and A. H. MacDonald for illuminating discussions. Part of this work was done at NHMFL; we thank G. Armstrong, T. Murphy, and E. Palm for support.

[1] J. F. Janak, Phys. Rev. **178**, 1416 (1969).
[2] T. Okamoto, K. Hosoya, S. Kawaji, and A. Yagi, Phys. Rev. Lett. **82**, 3875 (1999).
[3] S. A. Vitkalov, H. Zheng, K. M. Mertes, M. P. Sarachik, and T. M. Klapwijk, Phys. Rev. Lett. **87**, 086401 (2001).
[4] A. A. Shashkin, S. V. Kravchenko, V. T. Dolgopolov, and T. M. Klapwijk, Phys. Rev. Lett. **87**, 086801 (2001).
[5] V. M. Pudalov, M. E. Gershenson, H. Kojima, N. Butch, E. M. Dizhur, G. Brunthaler, A. Prinz, and G. Bauer, Phys. Rev. Lett. **88**, 196404 (2002).
[6] J. Zhu, H. L. Stormer, L. N. Pfeiffer, K. W. Baldwin, and K. W. West, Phys. Rev. Lett. **90**, 056805 (2003).
[7] E. Tutuc, S. Melinte, E. P. De Poortere, M. Shayegan, and R. Winkler, Phys. Rev. B **67**, 241309(R) (2003).
[8] Y. P. Shkolnikov, K. Vakili, E. P. De Poortere, and M. Shayegan, Phys. Rev. Lett. **92**, 246804 (2004).
[9] K. Vakili, Y. P. Shkolnikov, E. Tutuc, E. P. De Poortere, and M. Shayegan, Phys. Rev. Lett. **92**, 226401 (2004).
[10] O. Prus, Y. Yaish, M. Reznikov, U. Sivan, and V. Pudalov, Phys. Rev. B **67**, 205407 (2003).
[11] J. Yoon, C. C. Li, D. Shahar, D. C. Tsui, and M. Shayegan, Phys. Rev. Lett. **82**, 1744 (1999).
[12] S. J. Papadakis, E. P. De Poortere, M. Shayegan, and R. Winkler, Phys. Rev. Lett. **84**, 5592 (2000).
[13] E. Tutuc, E. P. De Poortere, S. J. Papadakis, and M. Shayegan, Phys. Rev. Lett. **86**, 2858 (2001).
[14] Y. Y. Proskuryakov, A. K. Savchenko, S. S. Safonov, M. Pepper, M. Y. Simmons, and D. A. Ritchie, Phys. Rev. Lett. **89**, 076406 (2002).
[15] H. Noh, M. P. Lilly, D. C. Tsui, J. A. Simmons, E. H. Hwang, S. Das Sarma, L. N. Pfeiffer, and K. W. West, Phys. Rev. B **68**, 165308 (2003).
[16] R. Winkler, Phys. Rev. B **70**, 125301 (2004).
[17] R. Winkler, Phys. Rev. B **71**, 113307 (2005).
[18] Y. Zhang and S. Das Sarma, Phys. Rev. B **72**, 075308 (2005).
[19] F. Bloch, Z. Phys. **57**, 545 (1929).
[20] E. C. Stoner, Proc. R. Soc. London, Ser. A **165**, 372 (1938).
[21] E. Abrahams, S. V. Kravchenko, and M. P. Sarachik, Rev. Mod.

Phys. **73**, 251 (2001).
[22] T. Dietl, H. Ohno, and F. Matsukura, Phys. Rev. B **63**, 195205 (2001).
[23] M. Abolfath, T. Jungwirth, J. Brum, and A. H. MacDonald, Phys. Rev. B **63**, 054418 (2001).
[24] R. Winkler, *Spin-Orbit Coupling Effects in Two-Dimensional Electron and Hole Systems* (Springer, Berlin, 2003), and references therein.
[25] In the calculations, the front and back gates are modeled by different boundary conditions for the Hartree potential.
[26] A. K. Rajagopal and J. C. Kimball, Phys. Rev. B **15**, 2819 (1977).
[27] B. Tanatar and D. M. Ceperley, Phys. Rev. B **39**, 5005 (1989).
[28] C. Attaccalite, S. Moroni, P. Gori-Giorgi, and G. B. Bachelet, Phys. Rev. Lett. **88**, 256601 (2002).
[29] H. W. van Kesteren, E. C. Cosman, W. A. J. A. van der Poel, and C. T. Foxon, Phys. Rev. B **41**, 5283 (1990).
[30] S. Y. Lin, H. P. Wei, D. C. Tsui, J. F. Klem, and S. J. Allen, Jr., Phys. Rev. B **43**, 12110 (1991).
[31] F. Stern, Phys. Rev. Lett. **21**, 1687 (1968).
[32] Electron data in Fig. 3 are from sample A of Ref. 7.
[33] W. Pan, K. Lai, S. P. Bayrakci, N. P. Ong, D. C. Tsui, L. N. Pfeiffer, and K. W. West, Appl. Phys. Lett. **83**, 3519 (2003).
[34] The multipoles are normalized such that the largest possible values are unity.
[35] Y.-W. Tan, J. Zhu, H. L. Stormer, L. N. Pfeiffer, K. W. Baldwin, and K. W. West, Phys. Rev. Lett. **94**, 016405 (2005).
[36] C. Kittel, *Quantum Theory of Solids* (Wiley, New York, 1963).
[37] F. Stern, Phys. Rev. Lett. **30**, 278 (1973).
[38] Calculations for model HH systems at $B>0$ (unpublished) suggest that we can have either a large dipole or a large octupole moment, consistent with Fig. 4.
[39] Similarly, a Fermi liquid theory for spin-3/2 particles depends on additional independent Fermi liquid parameters beyond those in the usual theory for spin-1/2 systems.
[40] A. H. MacDonald (private communication).
[41] Experimental data for sample Q2 are from Ref. 12. Within experimental accuracy, they are independent of the direction of the current.
[42] The large dipole of 2DHSs in an in-plane magnetic field $B_{[33\bar{2}]}$ is a consequence of the low symmetry of the (113) surface that results in a highly anisotropic Zeeman splitting of the 2DHS. Within the 2×2 subspace of HH states, the in-plane field $B_{[33\bar{2}]}$ gives rise to an off-diagonal Zeeman term $\propto B_{[33\bar{2}]}\sigma_z$, where σ_z is the Pauli spin matrix for the z direction perpendicular to the 2D plane (Ref. 24). So in this particular case, the in-plane field acts like a perpendicular field.